Exclusive multi-body Hadronic Decays of the $\psi(2S)^*$

Z. Li,[1] A. Lopez,[1] H. Mendez,[1] J. Ramirez,[1] G. S. Huang,[2] D. H. Miller,[2] V. Pavlunin,[2]
B. Sanghi,[2] E. I. Shibata,[2] I. P. J. Shipsey,[2] G. S. Adams,[3] M. Chasse,[3] M. Cravey,[3]
J. P. Cummings,[3] I. Danko,[3] J. Napolitano,[3] D. Cronin-Hennessy,[4] C. S. Park,[4]
W. Park,[4] J. B. Thayer,[4] E. H. Thorndike,[4] T. E. Coan,[5] Y. S. Gao,[5] F. Liu,[5]
M. Artuso,[6] C. Boulahouache,[6] S. Blusk,[6] J. Butt,[6] E. Dambasuren,[6] O. Dorjkhaidav,[6]
N. Menaa,[6] R. Mountain,[6] H. Muramatsu,[6] R. Nandakumar,[6] R. Redjimi,[6] R. Sia,[6]
T. Skwarnicki,[6] S. Stone,[6] J. C. Wang,[6] K. Zhang,[6] S. E. Csorna,[7] G. Bonvicini,[8]
D. Cinabro,[8] M. Dubrovin,[8] R. A. Briere,[9] G. P. Chen,[9] T. Ferguson,[9] G. Tatishvili,[9]
H. Vogel,[9] M. E. Watkins,[9] N. E. Adam,[10] J. P. Alexander,[10] K. Berkelman,[10]
D. G. Cassel,[10] J. E. Duboscq,[10] K. M. Ecklund,[10] R. Ehrlich,[10] L. Fields,[10]
R. S. Galik,[10] L. Gibbons,[10] B. Gittelman,[10] R. Gray,[10] S. W. Gray,[10] D. L. Hartill,[10]
B. K. Heltsley,[10] D. Hertz,[10] L. Hsu,[10] C. D. Jones,[10] J. Kandaswamy,[10] D. L. Kreinick,[10]
V. E. Kuznetsov,[10] H. Mahlke-Krüger,[10] T. O. Meyer,[10] P. U. E. Onyisi,[10]
J. R. Patterson,[10] D. Peterson,[10] J. Pivarski,[10] D. Riley,[10] J. L. Rosner,[10, †] A. Ryd,[10]
A. J. Sadoff,[10] H. Schwarthoff,[10] M. R. Shepherd,[10] W. M. Sun,[10] J. G. Thayer,[10]
D. Urner,[10] T. Wilksen,[10] M. Weinberger,[10] S. B. Athar,[11] P. Avery,[11] L. Breva-Newell,[11]
R. Patel,[11] V. Potlia,[11] H. Stoeck,[11] J. Yelton,[11] P. Rubin,[12] B. I. Eisenstein,[13]
G. D. Gollin,[13] I. Karliner,[13] D. Kim,[13] N. Lowrey,[13] P. Naik,[13] C. Sedlack,[13]
M. Selen,[13] J. J. Thaler,[13] J. Williams,[13] J. Wiss,[13] K. W. Edwards,[14] D. Besson,[15]
K. Y. Gao,[16] D. T. Gong,[16] Y. Kubota,[16] B.W. Lang,[16] S. Z. Li,[16] R. Poling,[16]
A. W. Scott,[16] A. Smith,[16] C. J. Stepaniak,[16] J. Urheim,[16] Z. Metreveli,[17] K. K. Seth,[17]
A. Tomaradze,[17] P. Zweber,[17] J. Ernst,[18] A. H. Mahmood,[18] H. Severini,[19]
D. M. Asner,[20] S. A. Dytman,[20] S. Mehrabyan,[20] J. A. Mueller,[20] and V. Savinov[20]

(CLEO Collaboration)

[1] *University of Puerto Rico, Mayaguez, Puerto Rico 00681*
[2] *Purdue University, West Lafayette, Indiana 47907*
[3] *Rensselaer Polytechnic Institute, Troy, New York 12180*
[4] *University of Rochester, Rochester, New York 14627*
[5] *Southern Methodist University, Dallas, Texas 75275*
[6] *Syracuse University, Syracuse, New York 13244*
[7] *Vanderbilt University, Nashville, Tennessee 37235*
[8] *Wayne State University, Detroit, Michigan 48202*
[9] *Carnegie Mellon University, Pittsburgh, Pennsylvania 15213*
[10] *Cornell University, Ithaca, New York 14853*
[11] *University of Florida, Gainesville, Florida 32611*
[12] *George Mason University, Fairfax, Virginia 22030*
[13] *University of Illinois, Urbana-Champaign, Illinois 61801*
[14] *Carleton University, Ottawa, Ontario, Canada K1S 5B6
and the Institute of Particle Physics, Canada*
[15] *University of Kansas, Lawrence, Kansas 66045*
[16] *University of Minnesota, Minneapolis, Minnesota 55455*
[17] *Northwestern University, Evanston, Illinois 60208*
[18] *State University of New York at Albany, Albany, New York 12222*

[19]*University of Oklahoma, Norman, Oklahoma 73019*
[20]*University of Pittsburgh, Pittsburgh, Pennsylvania 15260*

(Dated: February 7, 2008)

Abstract

Using data accumulated with the CLEO detector corresponding to an integrated luminosity of $\mathcal{L}$=5.46 pb^{-1} on the peak of the $\psi(2S)$ and 20.46 pb^{-1} at $\sqrt{s}$=3.67 GeV, we report preliminary branching fraction measurements for seven new decay modes of the $\psi(2S)$ ($\eta 3\pi$, $\eta' 3\pi$, $2(K^+ K^-)$, $p\bar{p}K^+ K^-$, $\Lambda\bar{\Lambda}\pi^+\pi^-$, $\Lambda\bar{p}K^+$, and $\Lambda\bar{p}K^+\pi^+\pi^-$) and more precise measurements of nine previously measured modes ($2(\pi^+\pi^-)$, $2(\pi^+\pi^-)\pi^0$, $\omega\pi^+\pi^-$, $K^+K^-\pi^+\pi^-$, $\phi\pi^+\pi^-$, ωK^+K^-, ϕK^+K^-, $p\bar{p}\pi^+\pi^-$, and $\Lambda\bar{\Lambda}$). We also include a study of $\omega p\bar{p}$ and obtain an improved upper limit for $\phi p\bar{p}$. Results are compared, where possible, with the corresponding J/ψ branching ratios to test the 12% rule.

In perturbative QCD the states J/ψ and $\psi(2S)$ are non-relativistic bound states of a charm and an anti-charm quark. The decays of these states are expected to be dominated by the annihilation of the constituent $c\bar{c}$ into three gluons. The partial width for the decays into an exclusive hadronic state, h, is expected to be proportional to the square of the $c\bar{c}$ wave function overlap at the origin, which is well determined from the leptonic width [1]. Since the strong coupling constant, α_s, is not very different at the J/ψ and $\psi(2S)$ masses, it is expected that for any state h the J/ψ and $\psi(2S)$ branching ratios are related by [2]

$$Q_h = \frac{\mathcal{B}(\psi(2S) \to h)}{\mathcal{B}(J/\psi \to h)} \approx \frac{\mathcal{B}(\psi(2S) \to \ell^+\ell^-)}{\mathcal{B}(J/\psi \to \ell^+\ell^-)} = (12.7 \pm 0.5)\%, \qquad (1)$$

where $\mathcal{B}$ denotes a branching fraction, h is a particular hadronic final state, and the leptonic branching fractions are taken from the PDG [1]. This relation is sometimes called "the 12% rule". Modest deviations from the rule are expected [3]. Although the rule works well for some specific decay modes of the $\psi(2S)$, it fails spectacularly for $\psi(2S)$ decays to final states consisting of one vector and one pseudoscalar meson, such as $\rho\pi$.

Values of Q_h have been measured for a wide variety of final states [1, 4, 5]. Most recently CLEO has measured additional 1^-0^- final states at the $\psi(2S)$ and the continuum [6], including the first observation of $\psi(2S) \to \rho\pi$. A recent review [3] of relevant theory and experiment concludes that current theoretical explanations are unsatisfactory. Clearly more experimental results are desirable. This paper presents measurements of the following new decay modes of the $\psi(2S)$: $\eta 3\pi$, $\eta' 3\pi$, $2(K^+K^-)$, $p\bar{p}K^+K^-$, $\Lambda\bar{\Lambda}\pi^+\pi^-$, $\Lambda\bar{p}K^+$, $\Lambda\bar{p}K^+\pi^+\pi^-$, and more precise measurements of these previously measured modes: $2(\pi^+\pi^-)$, $2(\pi^+\pi^-)\pi^0$, $\omega\pi^+\pi^-$, $K^+K^-\pi^+\pi^-$, $\phi\pi^+\pi^-$, ωK^+K^-, ϕK^+K^-, $p\bar{p}\pi^+\pi^-$, and $\Lambda\bar{\Lambda}$. We also measure $\omega p\bar{p}$ and obtain an improved upper limit for $\phi p\bar{p}$. Where applicable, the inclusion of charge conjugate modes is implied. Eleven of the modes we study have been previously observed at the J/ψ.

The data sample used in this analysis is obtained at the $\psi(2S)$ and the nearby continuum in e^+e^- collisions produced by the Cornell Electron Storage Ring (CESR) and acquired with the CLEO detector. The CLEO III detector [7] features a solid angle coverage for charged and neutral particles of 93%. The charged particle tracking system, operating in a 1.0 T magnetic field along the beam axis, achieves a momentum resolution of $\sim 0.6\%$ at $p = 1\,\text{GeV}/c$. The calorimeter attains a photon energy resolution of 2.2% at $E_\gamma = 1$ GeV and 5% at 100 MeV. Two particle identification systems, one based on energy loss (dE/dx) in the drift chamber and the other a ring-imaging Cherenkov (RICH) detector, are used together to separate $K^\pm$ from $\pi^\pm$. The combined dE/dx-RICH particle identification procedure has efficiencies exceeding 90% and misidentification rates below 5% for both $\pi^\pm$ and $K^\pm$.

Half of the $\psi(2S)$ data and all the continuum data were taken after a transition to the CLEO-c [8] detector configuration, in which CLEO III's silicon-strip vertex detector was replaced with a six-layer all-stereo drift chamber. The two detector configurations also correspond to different accelerator lattices: the former with a single wiggler magnet and a center-of-mass energy spread of 1.5 MeV, the latter (CESR-c [8]) with six wiggler magnets and an energy spread of 2.3 MeV.

The integrated luminosity ($\mathcal{L}$) of the datasets was measured using $\gamma\gamma$ events in the calorimeter [9]. Event counts were normalized with a Monte Carlo (MC) simulation based on the Babayaga [10] event generator combined with GEANT-based [11] detector modeling. The datasets consist of $\mathcal{L}=5.46$ pb^{-1} on the peak of the $\psi(2S)$ (2.57 pb^{-1} for CLEO III, 2.89 pb^{-1} for CLEO-c) and 20.46 pb^{-1} at $\sqrt{s}=3.67$ GeV (all CLEO-c). The nominal scale

factor used to normalize continuum yields to $\psi(2S)$ data is $f_{\text{nom}} = 0.2645 \pm 0.004$, and is determined from the integrated luminosities of the data sets corrected for the $1/s$ dependence of the cross section, where the error is from the relative luminosity uncertainty. The actual f used for each mode also corrects for the small differences in efficiency between the $\psi(2S)$ and continuum data samples.

Standard requirements are used to select charged particles reconstructed in the tracking system and photon candidates in the CsI calorimeter. We require tracks of charged particles to have momenta $p > 100$ MeV and to satisfy $|\cos\theta| < 0.90$, where θ is the polar angle with respect to the e^+ direction. Each photon candidate satisfies $E_\gamma > 30$ MeV and is more than 8 cm away from the projections of tracks into the calorimeter. Particle identification from dE/dx and the RICH is used on all charged particle candidates. Pions, kaons, and protons must be positively and uniquely identified. That is: pions must not satisfy interpretation as kaons or protons, and kaons and protons obey similar requirements. Charged particles must not be identified as electrons using criteria based on momentum, calorimeter energy deposition, and dE/dx.

The invariant mass of the decay products from the following particles must lie within limits determined from MC studies: π^0 ($M_{\gamma\gamma} = 120 - 150$ MeV), η ($M_{\gamma\gamma} = 500 - 580$ MeV), η ($M_{\pi^+\pi^-\pi^0} = 530 - 565$ MeV), ω ($M_{\pi^+\pi^-\pi^0} = 740 - 820$ MeV [$M_{\pi^+\pi^-\pi^0} = 760 - 800$ MeV for the $\omega p\bar{p}$ final state]), ϕ ($M_{K^+K^-} = 1.00 - 1.04$ GeV), and Λ ($M_{p\pi^-} = 1.1136 - 1.1180$ GeV). For $\pi^0 \to \gamma\gamma$ and $\eta \to \gamma\gamma$ candidates in events with more than two photons, the combination giving a mass closest to the known π^0 or η mass is chosen, and a kinematically constrained fit to the known parent mass is used. Fake π^0's and η's are suppressed with lateral electromagnetic shower profile restrictions. For $\eta \to \pi^+\pi^-\pi^0$ and $\omega \to \pi^+\pi^-\pi^0$, the π^0 is selected as described above, and then combined with all possible combinations of two oppositely charged pions choosing the combination that is closest to the $\eta(\omega)$ mass. A kinematically constrained fit is used for neither of these modes, nor for ϕ's or for Λ's. For $\Lambda \to p\pi^-$, a fit of the $p\pi^-$ trajectories to a common vertex separated from the e^+e^- interaction ellipsoid is made. Contamination from K_S decays is eliminated primarily by the energy and momentum requirements imposed on the event, and by particle identification.

Energy and momentum conservation requirements are imposed on the reconstructed final state hadrons, which have momentum p_i and combined measured energy E_{vis}. We require the measured scaled energy $E_{\text{vis}}/E_{\text{cm}}$ be consistent with unity within experimental resolution, which varies by final state. We require $|\Sigma\mathbf{p_i}|/E_{\text{cm}} < 0.02$. Together these requirements suppress backgrounds with missing energy or incorrect mass assignments. The experimental resolutions are smaller than 1% in scaled energy and 2% in scaled momentum.

For the final states $2(\pi^+\pi^-)\pi^0$, $\omega\pi^+\pi^-$, and ωK^+K^-, an additional cut is applied to remove a background of radiative events. When the photon is combined with a low-energy photon signal, it can imitate a π^0. We require $(E_{\text{4tracks}} + E_\gamma)/E_{\text{cm}} < 0.995$, where E_γ is the energy of the highest energy photon.

In order to compute Q_h in modes with two or more charged pions, two π^0's or an η, it is necessary to remove the contribution from the transitions $\psi(2S) \to J/\psi X$, where $X = \pi^+\pi^-$, $\pi^0\pi^0$, or η [12]. Accordingly we reject events in which the mass of any of the following falls within the range $3.05 < m < 3.15$ GeV: the two highest momentum oppositely charged tracks, the recoil mass against the two lowest momentum oppositely charged tracks, or the mass recoiling against the $2\pi^0$'s or η.

For every final state, a signal selection range in $E_{\text{vis}}/E_{\text{cm}}$ is determined by Monte Carlo simulation, and a sideband selection range is defined to measure background. Final states

with the intermediate η, ω, or ϕ particles must satisfy a scaled energy signal selection range requirement identical to the corresponding mode without the intermediate particle. For example, the scaled energy signal selection range is the same for $\phi K^+ K^-$ and $K^+ K^- K^+ K^-$. For final states with an η, ω, or ϕ, the event yield is determined from signal and sideband selection ranges of the intermediate particle mass. The scaled energy and mass signal and sideband selection ranges for $\psi(2S)$ and continuum data are identical, and are listed by mode in Tables I and II.

TABLE I: Signal and sideband selection ranges for the scaled energy, $E_{\mathrm{vis}}/E_{\mathrm{cm}}$, by mode.

mode	signal	sideband
$2(\pi^+\pi^-)$	0.98-1.02	0.96-0.98, 1.02-1.04
$2(\pi^+\pi^-)\pi^0$	0.98-1.02	0.96-0.98, 1.02-1.04
$K^+K^-\pi^+\pi^-$	0.99-1.01	0.98-0.99, 1.01-1.02
$2(K^+K^-)$	0.99-1.01	0.98-0.99, 1.01-1.02
$p\bar{p}\pi^+\pi^-$	0.99-1.01	0.98-0.99, 1.01-1.02
$p\bar{p}K^+K^-$	0.99-1.01	0.98-0.99, 1.01-1.02
$\Lambda\bar{\Lambda}$	0.99-1.01	0.98-0.99, 1.01-1.02
$\Lambda\bar{\Lambda}\pi^+\pi^-$	0.99-1.01	0.98-0.99, 1.01-1.02
$\Lambda\bar{p}K^+$	0.99-1.01	0.98-0.99, 1.01-1.02
$\Lambda\bar{p}K^+\pi^+\pi^-$	0.99-1.01	0.98-0.99, 1.01-1.02

TABLE II: The mass signal and sideband selection ranges for modes with an η, ω, or ϕ. Modes with these particles must satisfy a scaled energy signal selection requirement identical to the corresponding mode without the intermediate particle.

mode	Variable	signal (GeV)	sideband (GeV)
$\omega\pi^+\pi^-$	$m_{3\pi}$	0.74-0.82	0.70-0.74, 0.82-0.86
ωK^+K^-	$m_{3\pi}$	0.74-0.82	0.70-0.74, 0.82-0.86
$\omega p\bar{p}$	$m_{3\pi}$	0.76-0.80	0.74-0.76, 0.80-0.82
$\eta^{\to\gamma\gamma}3\pi$	$m_{\gamma\gamma}$	0.50-0.58	0.455-0.50,0.58-0.615
$\eta^{\to\pi^+\pi^-\pi^0}3\pi$	$m_{3\pi}$	0.530-0.565	0.51-0.53,0.565-0.58
$\eta'3\pi$	$m_{\pi\pi\gamma\gamma}$	0.945-0.970	0.9325-0.945,0.97-0.9825
$\phi\pi^+\pi^-$	$m_{K^+K^-}$	1.00-1.04	1.04-1.08
ϕK^+K^-	$m_{K^+K^-}$	1.00-1.04	1.04-1.08
$\phi p\bar{p}$	$m_{K^+K^-}$	1.00-1.04	1.04-1.08

Figures 1 and 2 show the distributions of $E_{\rm vis}/E_{\rm cm}$ and resonance mass, where relevant, for all final states. The $\psi(2S)$ data is represented by the points with error bars, the open histogram is signal Monte Carlo with arbitrary normalization, and the shaded histogram is the scaled continuum. The arrows indicate the scaled energy and resonance mass selection ranges. The requirements of energy and momentum conservation together with particle identification result in small backgrounds. The dominant background in most modes at the $\psi(2S)$ is from the continuum.

Event totals are shown for both the $\psi(2S)$ and the continuum in Table III, where $S_{\psi(2S)}$ (S_{co}) is the number of events in the signal region and $B_{\psi(2S)}$ (B_{co}) the number of events in the sideband region in $\psi(2S)$ (continuum) data. Under the assumption that interference between $\psi(2S)$ decay and continuum production of the same final state is absent, the number of events attributable to each $\psi(2S)$ decay mode, N_S, is

$$N_S = S_{\psi(2S)} - B_{\psi(2S)} - f(S_{co} - B_{co}), \qquad (2)$$

where f is mode dependent and listed in Table III. We observe a statistically significant signal in all modes except $\phi p\bar{p}$. The signal with the least statistical significance is $\omega p\bar{p}$ (4.7σ).

The efficiency, ϵ, for each final state is the average obtained from MC simulations [11] for both detector configurations; the two values are typically within a few percent (relative) to each other. No initial state radiation is included in the Monte Carlo, but final state radiation is accounted for. The efficiencies in Table III include the branching ratios for intermediate final states.

We correct N_S for the efficiency and normalize to the number of $\psi(2S) \to \pi^+\pi^- J/\psi$, $J/\psi \to \mu^+\mu^-$ decays in the data, which has been determined previously to be $(6.75 \pm 0.12) \times 10^4$, where the error accounts for data and MC statistics (0.7%) and for uncertainties in trigger efficiency (0.5%) and angular distributions (1.5%). Complete details may be found in [6]. The resulting relative branching ratios are listed in Table III. The absolute branching ratios are determined using $\mathcal{B}(\psi(2S) \to \pi^+\pi^- J/\psi) = 0.323 \pm 0.013$ [1] and $\mathcal{B}(J/\psi \to \mu^+\mu^-) = (5.88 \pm 0.10)\%$ [1]. Q_h values are determined using the absolute $\psi(2S)$ branching ratios determined in this analysis and J/ψ branching ratios from [1].

The systematic errors on the ratio of branching fractions share common contributions from the number of $\psi(2S) \to \pi^+\pi^- J/\psi$, $J/\psi \to \mu^+\mu^-$ decays (1.7%), uncertainty in f (1.5%), trigger efficiency (1%), electron veto (1%), and Monte Carlo statistics (2%). Other sources vary by channel. We include the following contributions for detector performance modeling quality: charged particle tracking (3% per track), π^0/η finding (4.4%), Λ finding (3%), $\pi/K/p$ identification (1%/ identified $\pi/K/p$), and scaled energy and mass resolutions (2%). The systematic error associated with the uncertainty in the level of background is obtained by recomputing the branching ratio when the background at the $\psi(2S)$ and the continuum are coherently increased by 1σ. Since the background in many modes is small, the Poisson probability for the observed number of background events to fluctuate up to the 68% C.L. value is calculated and interpreted as the uncertainty in the level of background. The efficiencies were determined using events generated according to phase space. Many of the modes studied may have resonant submodes. A preliminary analysis finds the following prominent examples: $2(\pi^+\pi^-)$ where $\rho\pi\pi$ is dominant, $\omega\pi\pi$ where $b_1\pi$ is dominant and $\omega f_2(1270)$ is significant, $K^+K^-\pi^+\pi^-$ where $K^*(892)K\pi$ and ρK^+K^- are large and $\phi\pi^+\pi^-$ is small, and $\eta 3\pi$ where $\eta\pi^0\rho^0$, $\eta\rho^+\pi^-$, and $\eta\rho^-\pi^+$ dominate. Allowing for the presence of resonant submodes changes the efficiency by less than 5% relative to the non-resonant efficiency for each mode we have studied. To account for this and the possibility of
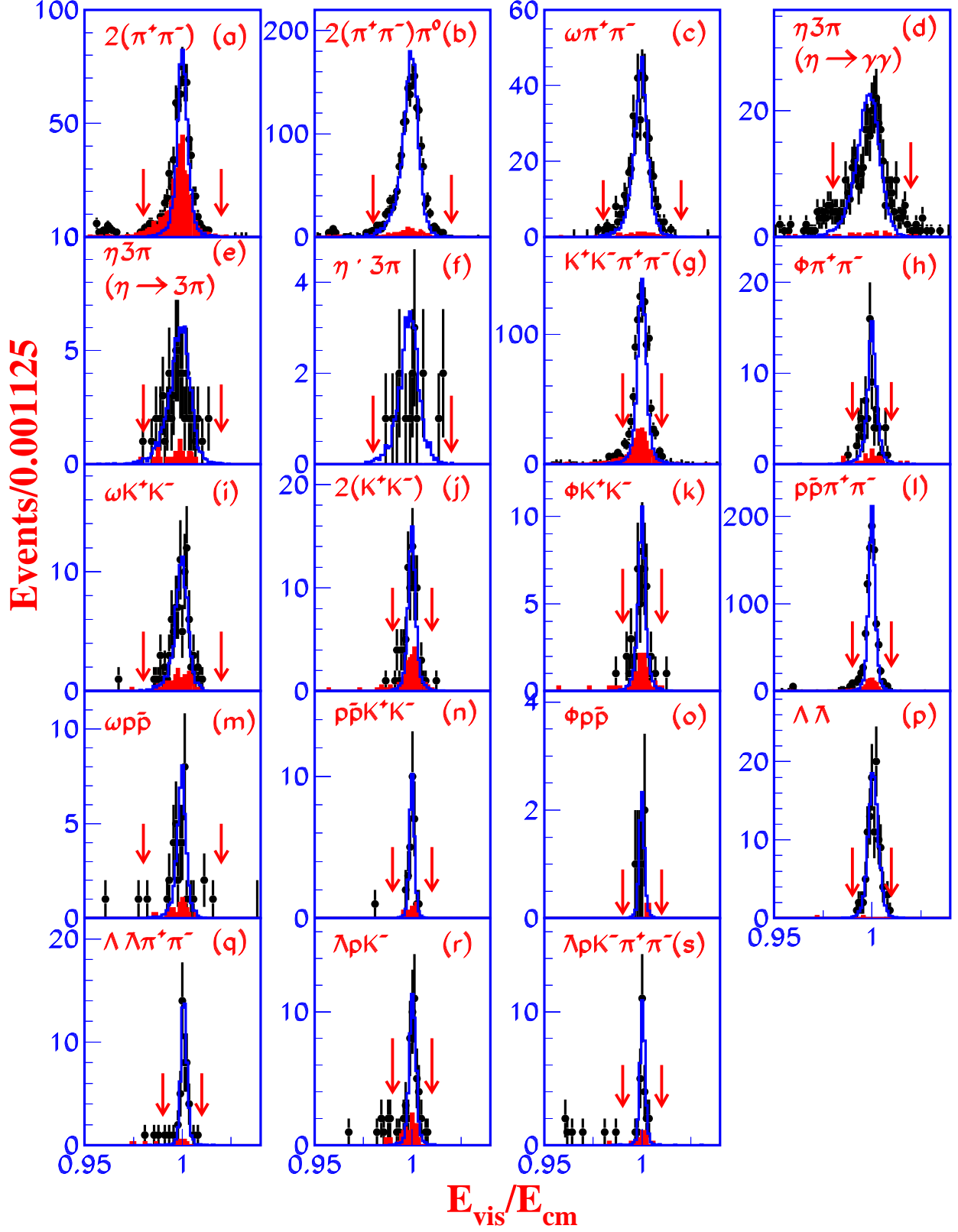
FIG. 1: Distributions of the scaled visible energy E_{vis}/E_{cm} for labeled final states. In each figure, entries are shown for $\psi(2S)$ data (points with error bars), signal Monte Carlo with arbitrary normalization (open histogram), and scaled continuum (shaded histogram). The vertical arrows indicate ends of signal selection ranges.
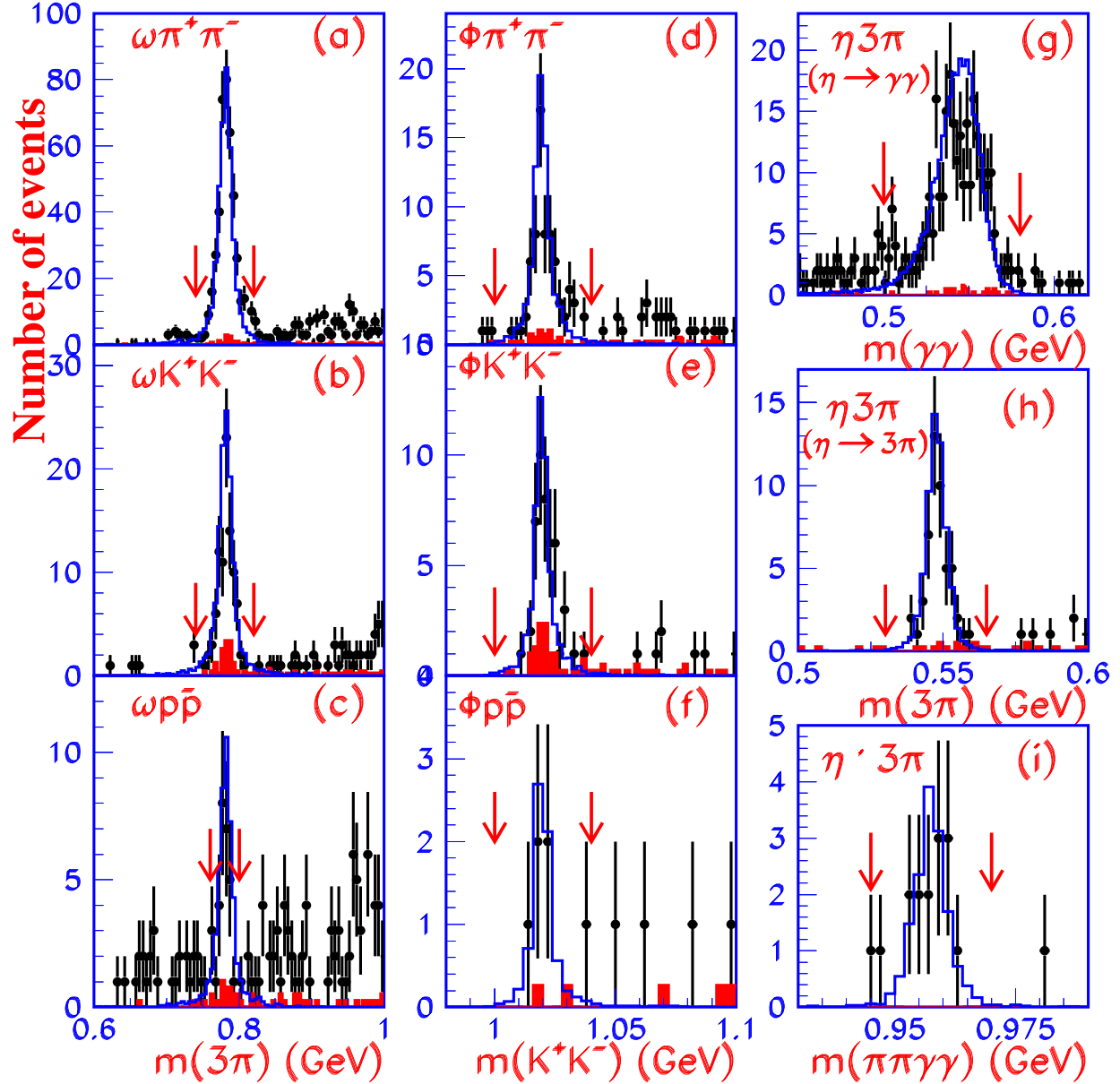
FIG. 2: Distributions of the intermediate particle mass for labeled final states. In each figure, entries are shown for $\psi(2S)$ data (points with error bars), signal Monte Carlo with arbitrary normalization (open histogram) and scaled continuum (shaded histogram). The vertical arrows indicate ends of signal selection ranges.

resonance polarization, we assign a 10% modeling systematic error to all modes. Systematic uncertainties are significant for all modes and the dominant error for many.

Figure 3 shows the branching ratios measured in this analysis and a comparison to previous measurements [1]. In Table IV the values of Q_h for those final states with measured branching ratios at the J/ψ [1] are given. Figure 4 shows the Q_h values from Table IV and a comparison to previous measurements. This is the first measurement of $Q_{\Lambda\bar{p}K}$. The values of Q_h appear to be independent of the final state with no significant differences between

TABLE III: For each final state h: the number of events in the signal region, S_{co}, and background from sidebands, B_{co}, in continuum data; the scale factor, f; the number of events in the signal region, $S_{\psi(2S)}$, and background from sidebands, $B_{\psi(2S)}$, in $\psi(2S)$ data; the number of events attributable to $\psi(2S)$ decay, N_S, computed according to Equation (2); the average efficiency, ϵ; the ratio $\mathcal{B}(\psi(2S) \to h)/\mathcal{B}(\psi(2S) \to \pi^+\pi^- J/\psi, J/\psi \to \mu^+\mu^-)$ and the absolute branching fraction with statistical (68% C.L.) and systematic errors. For $\eta 3\pi$, the two decays modes $\eta \to \gamma\gamma$ and $\eta \to 3\pi$ are combined on line $\eta 3\pi$. The branching ratios reported here explicitly exclude contributions from $\psi(2S) \to J/\psi X$, where $X = \pi^+\pi^-$, $\pi^0\pi^0$, or η.

mode h	S_{co}	B_{co}	f	$S_{\psi(2S)}$	$B_{\psi(2S)}$	N_S	ϵ	$\dfrac{\mathcal{B}(\psi(2S)\to h)}{\mathcal{B}^{\psi(2S)}_{\pi^+\pi^-J/\psi}\mathcal{B}^{J/\psi}_{\mu^+\mu^-}}$ (10^{-4})	$\mathcal{B}(\psi(2S) \to h)$ (10^{-4})
$2(\pi^+\pi^-)$	1437	39	0.2680	700	19	306.3	0.4317	$105.1 \pm 11.5 \pm 13.6$	$2.0 \pm 0.2 \pm 0.3$
$2(\pi^+\pi^-)\pi^0$	343	28	0.2549	1742	39	1622.7	0.1927	$1247.1 \pm 46.2 \pm 171.3$	$23.7 \pm 0.6 \pm 3.3$
$\omega\pi^+\pi^-$	45	7	0.2412	426	38	378.8	0.1338	$419.5 \pm 33.7 \pm 58.5$	$8.0 \pm 0.5 \pm 1.1$
$\eta^{\to\gamma\gamma}3\pi$	28	2	0.2507	271	49	215.5	0.0595	$536.8 \pm 62.8 \pm 92.6$	$10.2 \pm 0.8 \pm 1.8$
$\eta^{\to\pi^+\pi^-\pi^0}3\pi$	19	10	0.2676	50	1	46.6	0.0186	$370.2 \pm 66.8 \pm 59.1$	$7.0 \pm 1.1 \pm 1.3$
$\eta 3\pi$									$8.5 \pm 0.7 \pm 1.6$
$\eta'3\pi$	0	0	0.2349	14	2	12.0	0.0079	$225.1 \pm 113.9 \pm 69.9$	$4.3 \pm 1.5 \pm 1.2$
$K^+K^-\pi^+\pi^-$	825	103	0.2694	1018	49	774.5	0.3372	$340.2 \pm 20.6 \pm 44.0$	$6.5 \pm 0.3 \pm 0.8$
$\phi\pi^+\pi^-$	26	12	0.2738	72	18	50.2	0.1545	$48.1 \pm 15.7 \pm 9.9$	$0.9 \pm 0.2 \pm 0.2$
ωK^+K^-	57	11	0.2091	92	8	74.4	0.1110	$99.3 \pm 17.8 \pm 14.8$	$1.9 \pm 0.3 \pm 0.3$
$2(K^+K^-)$	100	10	0.2727	81	2	54.5	0.2605	$31.0 \pm 8.4 \pm 4.6$	$0.6 \pm 0.1 \pm 0.1$
ϕK^+K^-	45	16	0.2729	46	4	34.1	0.1331	$37.9 \pm 12.2 \pm 6.8$	$0.7 \pm 0.2 \pm 0.1$
$p\bar{p}\pi^+\pi^-$	328	31	0.2552	963	31	856.2	0.4481	$283.0 \pm 14.5 \pm 36.5$	$5.4 \pm 0.2 \pm 0.7$
$\omega p\bar{p}$	18	5	0.2314	29	8	18.0	0.1060	$25.1 \pm 11.4 \pm 6.8$	$0.5 \pm 0.2 \pm 0.1$
$p\bar{p}K^+K^-$	17	0	0.2563	29	1	23.6	0.3445	$10.2 \pm 3.2 \pm 1.7$	$0.2 \pm 0.1 \pm 0.1$
$\phi p\bar{p}$	2	1	0.2472	6	2	3.8	0.1242		< 0.18 (90%CL)
$\Lambda\bar{\Lambda}$	1	0	0.2431	112	0	111.8	0.1035	$160.0 \pm 19.9 \pm 22.8$	$3.0 \pm 0.3 \pm 0.4$
$\Lambda\bar{\Lambda}\pi^+\pi^-$	9	2	0.1775	46	3	41.8	0.0437	$141.4 \pm 27.1 \pm 26.6$	$2.7 \pm 0.5 \pm 0.6$
$\Lambda\bar{p}K^+$	38	5	0.2258	51	8	35.5	0.1429	$36.8 \pm 9.9 \pm 6.3$	$0.7 \pm 0.2 \pm 0.1$
$\Lambda\bar{p}K^+\pi^+\pi^-$	17	1	0.1370	26	2	21.8	0.0514	$62.8 \pm 23.6 \pm 15.0$	$1.2 \pm 0.3 \pm 0.3$

mesonic and baryonic modes. The data indicates that Q_h values are in general lower than the current leptonic ratio.

In summary, we have presented preliminary branching fractions for seven new decay modes of the $\psi(2S)$, namely $\eta 3\pi$, $\eta'3\pi$, $2(K^+K^-)$, $p\bar{p}K^+K^-$, $\Lambda\bar{\Lambda}\pi^+\pi^-$, $\Lambda\bar{p}K^+$, $\Lambda\bar{p}K^+\pi^+\pi^-$, and more precise measurements of nine previously measured modes, which are $2(\pi^+\pi^-)$, $2(\pi^+\pi^-)\pi^0$, $\omega\pi^+\pi^-$, $K^+K^-\pi^+\pi^-$, $\phi\pi^+\pi^-$, ωK^+K^-, ϕK^+K^-, $p\bar{p}\pi^+\pi^-$, and $\Lambda\bar{\Lambda}$. We also measure $\omega p\bar{p}$ and obtain an improved upper limit for $\phi p\bar{p}$. Results are compared, where possible, with the corresponding J/ψ branching ratios to test the 12% rule. This analysis is part of a comprehensive study of $\psi(2S)$ multi-body hadronic decays and their resonant substructure and is closely related to searches for non-$D\bar{D}$ decay modes of the $\psi(3770)$. Further results will be presented in the near future.
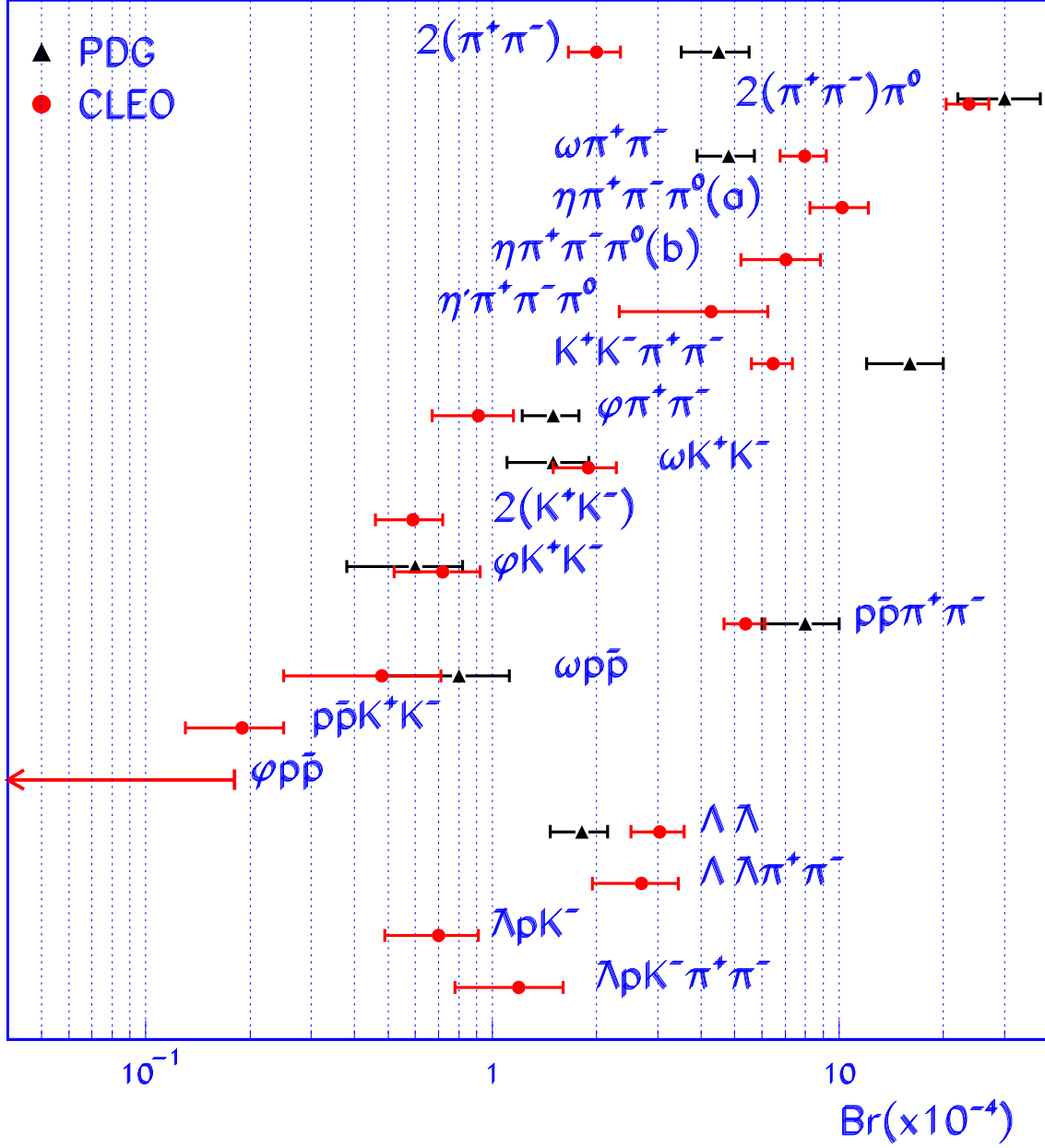
FIG. 3: A comparison of the measurements of the $\psi(2S)$ branching ratios for the labeled final states from this work (circles) and, when available, from the PDG [1] (triangles). The error bars are the quadrature sum of the statistical and systematic errors.
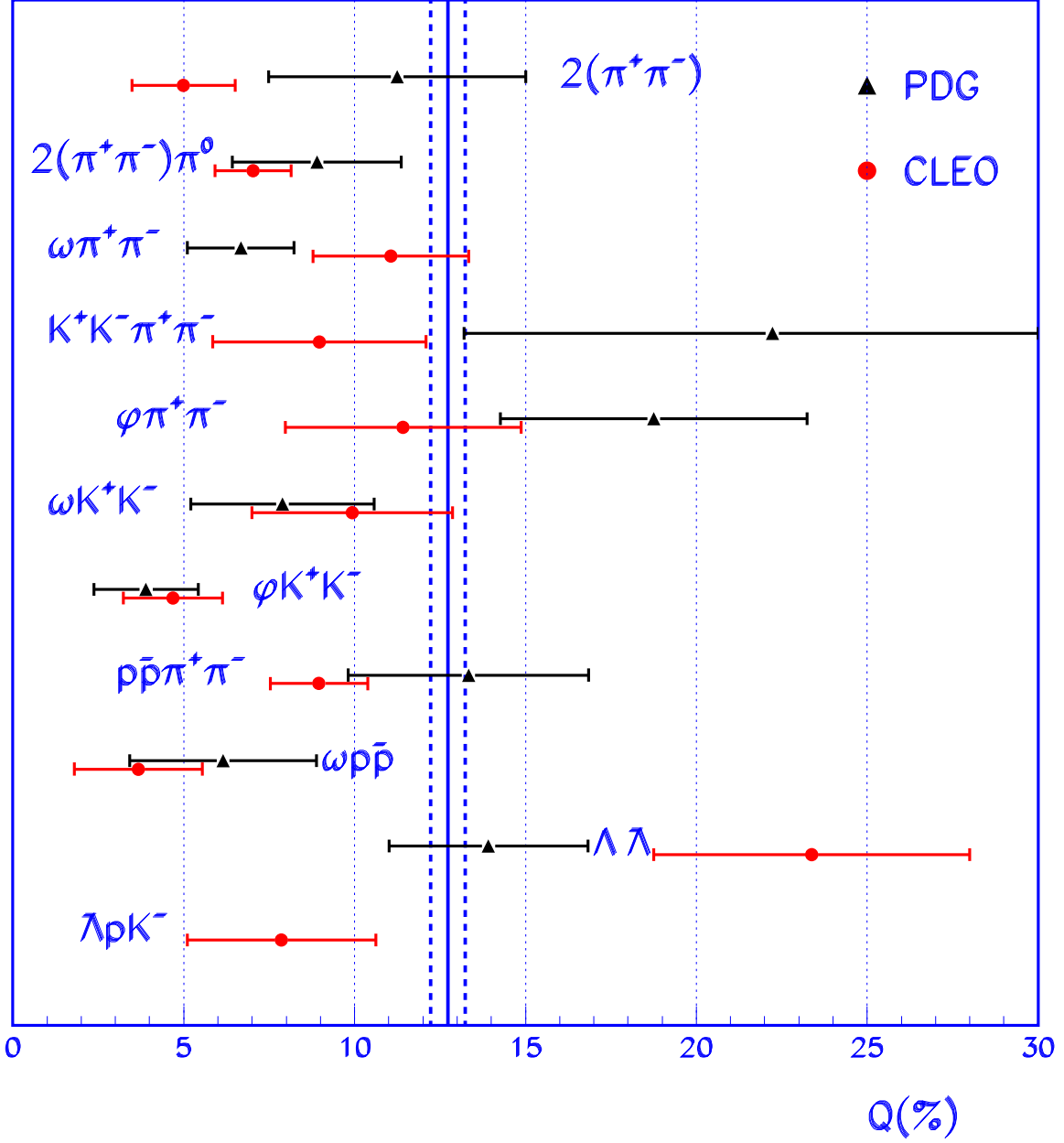
FIG. 4: A comparison of Q_h values for the labeled final states determined from the $\psi(2S)$ branching ratios measured in this work (circles) and J/ψ branching ratios from the PDG [1] to Q_h values determined from the PDG [1] (triangles). The error bars are the quadrature sum of the statistical and systematic errors. The current value of $Q_l = (12.7 \pm 0.5)\%$ [1] is displayed as the vertical solid line. The vertical dashed lines are the $\pm 1\sigma$ uncertainty in Q_l.

TABLE IV: For each final state h: the branching ratio from Table III, the corresponding branching ratio at the J/ψ from [1], and Q_h from Equation (1). The $\psi(2S)$ branching ratios and Q_h explicitly exclude contributions from $\psi(2S) \to J/\psi X$ where $X = \pi^+\pi^-$, $\pi^0\pi^0$, or η.

mode	$\mathcal{B}(\psi(2S) \to h)$ (10^{-4})		$Br(J/\psi)$ (10^{-4})	Q_h (%)
h	this work	PDG	PDG	this work
$2(\pi^+\pi^-)$	2.0 ± 0.3	4.5 ± 1.0	40 ± 10	5.0 ± 1.5
$2(\pi^+\pi^-)\pi^0$	23.7 ± 3.3	30 ± 8	337 ± 26	7.0 ± 1.1
$\omega\pi^+\pi^-$	8.0 ± 1.2	4.8 ± 0.9	72 ± 10	11.1 ± 2.3
$\eta 3\pi$	8.5 ± 1.0	-	-	-
$\eta' 3\pi$	4.3 ± 2.0	-	-	-
$K^+K^-\pi^+\pi^-$	6.5 ± 0.9	16 ± 4	72 ± 23	9.0 ± 3.1
$\phi\pi^+\pi^-$	0.9 ± 0.2	1.50 ± 0.28	8.0 ± 1.2	11.4 ± 3.5
ωK^+K^-	1.9 ± 0.4	1.5 ± 0.4	19 ± 4	9.9 ± 2.9
$2(K^+K^-)$	0.6 ± 0.1	-	-	-
ϕK^+K^-	0.7 ± 0.2	0.60 ± 0.22	15.4 ± 2.1	4.7 ± 1.6
$p\bar{p}\pi^+\pi^-$	5.4 ± 0.7	8.0 ± 2.0	60 ± 5	9.0 ± 1.4
$\omega p\bar{p}$	0.5 ± 0.2	0.80 ± 0.32	13 ± 2.5	3.7 ± 1.9
$p\bar{p}K^+K^-$	0.2 ± 0.1	-	-	-
$\phi p\bar{p}$	$< 0.18(90\%\text{CL})$	< 0.26	0.45 ± 0.15	-
$\Lambda\bar{\Lambda}$	3.0 ± 0.5	1.81 ± 0.34	13 ± 1.2	23.4 ± 4.6
$\Lambda\bar{\Lambda}\pi^+\pi^-$	2.7 ± 0.8	-	-	-
$\Lambda\bar{p}K^+$	0.7 ± 0.2	-	8.9 ± 1.6	7.9 ± 2.8
$\Lambda\bar{p}K^+\pi^+\pi^-$	1.2 ± 0.4	-	-	-

[1] Particle Data Group, S. Eidelman *et al.*, Phys. Lett. B **592**, 1 (2004).

[2] W. S. Hou and A. Soni, Phys. Rev. Lett. **50**, 569 (1983); G. Karl and W. Roberts, Phys. Lett. **B144**, 243 (1984); S. J. Brodsky *et al.*, Phys. Rev. Lett. **59**, 621 (1987); M. Chaichian *et al.*, Nucl. Phys. **B323**, 75 (1989); S. S. Pinsky, Phys. Lett. **B236**, 479 (1990); X. Q. Li *et al.*, Phys. Rev. **D55**, 1421 (1997); S. J. Brodsky and M. Karliner, Phys. Rev. Lett. **78**, 4682 (1997); Yu-Qi Chen and Eric Braaten, Phys. Rev. Lett. **80**, 5060 (1998); M. Suzuki, Phys. Rev. **D63**, 054021 (2001); J. L. Rosner, Phys. Rev. **D64**, 094002 (2001); J. P. Ma, Phys. Rev. **D65**, 097506 (2002); M. Suzuki, Phys. Rev. **D65**, 097507 (2002).

[3] Y.F. Gu and X.H. Li, Phys. Rev. D **63**, 114019 (2001).

[4] BES Collaboration, M. Ablikim *et al.*, arXiv:hep-ex/0407037, arXiv:hep-ex/0406038 (subm. to PLB), arXiv:hep-ex/0405050 (subm. to PRL), arXiv:hep-ex/0405030, and Phys. Rev. D **70**, 012003 (2004); BES Collaboration, J.Z. Bai *et al.*, Phys. Rev. D **70**, 012006 (2004) and Phys. Rev. D **69** 072001 (2004).

[5] F. A. Harris, arXiv:hep-ex/0407036 (subm. to Int. J. Mod. Phys. A).

[6] CLEO Collaboration, N.E. Adam *et al.*, arXiv:hep-ex/0407028 (subm. to PRL).

[7] CLEO Collaboration, Y. Kubota *et al.*, Nucl. Instrum. Methods Phys. Res., Sect. A **320**, 66 (1992); D. Peterson *et al.*, Nucl. Instrum. Methods Phys. Res., Sect. A **478**, 142 (2002); M. Artuso *et al.*, Nucl. Instrum. Methods Phys. Res., Sect. A **502**, 91 (2003).

[8] CLEO-c/CESR-c Taskforces & CLEO-c Collaboration, Cornell LEPP preprint CLNS 01/1742 (2001).

[9] CLEO Collaboration, G. Crawford *et al.*, Nucl. Instrum. Methods Phys. Res., Sect. A **345**, 429 (1992).

[10] C.M. Carloni Calame *et al.*, hep-ph/0312014 [in Proceedings of the Workshop on Hadronic Cross Section at Low Energy (SIGHAD03), Pisa, Italy, 2003 (to be published)].

[11] R. Brun *et al.*, GEANT 3.21, CERN Program Library Long Writeup W5013 (1993), unpublished.

[12] We do not veto J/ψ from $\psi(2S) \to J/\psi\pi^0$ since it is a very small contribution as $\mathcal{B}(\psi(2S) \to J/\psi\pi^0) = (9.6 \pm 2.1) \times 10^{-4}$.